

Anthro-X: Anthropomorphic Lower Extremity Exoskeleton Robot for Power Assistance

R.K.P.S. Ranaweera^{1*}, W.A.T.I. Jayasiri¹,

W.G.D. Tharaka¹, J.H.H.P. Gunasiri¹,

R.A.R.C. Gopura¹, T.S.S. Jayawardena²

Bionics Lab, Department of Mechanical Engineering¹

Department of Textile and Clothing Technology²

University of Moratuwa

Moratuwa 10400, Sri Lanka

e-mail: pubudur@uom.lk*

G.K.I. Mann

Faculty of Engineering and Applied Science

Memorial University of Newfoundland

Canada

Abstract—Lower extremity exoskeleton (LEE) robots are wearable devices that combine human intelligence with machine power to help perform functions of the limbs as intended by the user. Recently, anthropomorphic LEE solutions have gained wide spread interest to remedy the interference issues encountered at the human-robot interface. In that context, this paper presents a multi-degrees of freedom modular power-assist LEE robot with compatible joint axes to enhance kinematic compliance. The proposed LEE, named Anthro-X, supports all three DoF at the hip joint using a novel articulated mechanism. The polycentric motion of the knee joint is also facilitated using a unique mechanism based on four-bar linkage system. In total, Anthro-X has five DoF per limb where sagittal plane motions of hip and knee joints are powered by external power supply and others are passively supported. The prototype of the proposed LEE robot was fitted on a male subject to verify the kinematic conformity of hip and knee joint mechanisms. Experiments were then conducted to evaluate the effects of providing power assistance using Anthro-X during squatting exercises. Results indicate that the proposed design can be readily adapted for wide range of applications requiring motion or power assistance owing to its modular and anthropomorphic architecture.

Keywords—lower extremity exoskeleton robot; modular design; anthropomorphic architecture; power assistance

I. INTRODUCTION

Exoskeleton robots are wearable electromechanical devices that are designed to satisfy specific needs of the user. In essence the system should conform to the human's joints and limbs while working in parallel. Such robots are commonly classified according to the site of implementation such as upper extremity, lower extremity, full-body and other. The lower extremity exoskeleton (LEE) robots are generally developed for robotic rehabilitation, locomotion assistance, power augmentation and other niche applications [1]. In healthcare industry, medical LEE robots are increasingly used to regain functional mobility and/or to perform rehabilitation exercises of physically weak individuals such as elderly, injured or diseased. Similarly, able-bodied exoskeletons are mainly used for lift assisting and load carrying tasks. Although exoskeleton technology had matured over the years, issues arising from human-robot

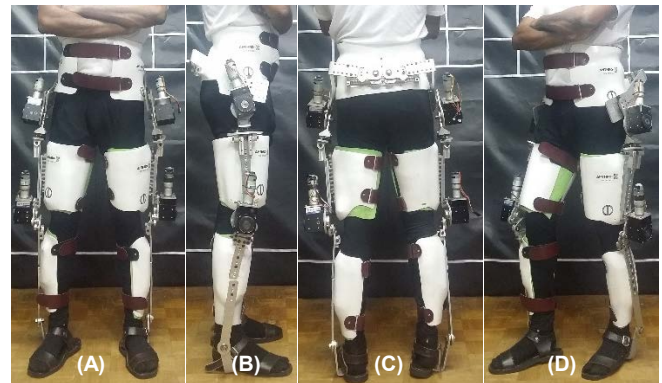


Figure 1. Prototype of Anthro-X fitted on 50th percentile male subject: (A) front view, (B) side view, (C) back view, (D) perspective view.

interaction need further attention [1]. One of the main reasons is the lack of conformity of exoskeleton joints and working axes to the biological counterparts [2]. The undue constraints imposed by the exoskeleton as a result of improper axes mapping may lead to poor muscle recruitment and hinder natural movement patterns of the limbs. Prolong usage may ultimately lead to higher overall energetic expenditure and cause injuries to the musculoskeletal system [3]. As such, this paper mainly covers design challenges, related work, mechanical design and experimental evaluation of novel mechanisms proposed for hip and knee joints. Objective is to develop an anthropomorphic LEE robot that can ensure safety, comfort and biomechanical performance.

II. DESIGN CHALLENGES

Anthro-X (See Fig. 1) is developed to provide power assistance to able-bodied users as well as motion assistance for patients suffering from muscle deterioration or neurological disorders. In case of able-bodied users, possible application areas include load lifting and load carrying. It can also be customized to help physiotherapists to conduct rehabilitation exercises for patients suffering with mobility disorders. Consequently, a multi-purpose LEE robot requiring superior kinematic conformity, has a broader range of design requirements to satisfy. In this pursuit, this section presents the anatomical and functional considerations relevant to LEE robot development.

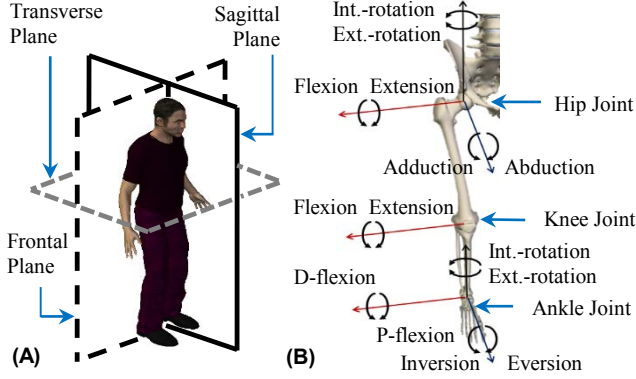


Figure 2. Human leg: (A) anatomical planes, (B) joints and motions.

A. Anatomical Considerations

Since primary activity of lower extremity is walking or ambulation, role of human anatomy for generation of associated movements needs to be studied. Human leg has three main joints and seven major degrees of freedom (DoF) excluding articulations at the foot [4]. Motions about each joint are defined with respect to the three anatomical planes, namely sagittal, frontal and transverse planes (See Fig. 2(B)). There are three DoF at hip joint, one DoF at knee joint, and three DoF at ankle joint (See Fig. 2(B)). As per the human anatomy, a given joint of the leg exhibit rotations about all planes during walking or ambulation [4]. Although the most significant motion of each joint, named flexion/extension, is recorded over the sagittal plane, motions about the frontal and transverse planes are also equally important from biomechanical and ergonomical points of view.

Hip joint formed between the pelvis and the femur bone represents a spherical joint. Here, the hip internal/external rotation facilitates the body to turn in the direction of walking [5]. In addition, both pelvic and hip rotations acts to decrease the vertical displacement of center of mass of the body and increase the stride length during walking. Similarly, hip abduction/adduction is crucial to maintain the balance when walking. Thus accurate mapping of the axes of rotations (AoR) of exoskeleton with biological hip joint is essential to further improve the agility, stability and biomechanical performance of the user. As a result, exoskeleton designs that restrict triplanar motions at hip joint are unsuccessful in meeting the motion intentions of the user. Considering the role of hip joint for propulsion, the overall biomechanical energetic expenditure can also significantly increase if the hip joint and pelvis are excessively restricted.

Knee joint complex consists two main joints, namely tibiofemoral joint and patellofemoral joint, to facilitate flexion/extension. However, relative sliding and rolling between tibia and femur bones results in displacement of the AoR of the knee. The behavior is referred to as ‘moving axis of rotation’ or ‘polycentric motion’ of the knee joint [4, 5]. If the mechanism is rigidly attached to biological knee, misalignment of AoR can cause undue interference and discomfort to the user. As such, the generic exoskeleton designs with revolute joints or fixed AoR can inhibit the natural range of motion of knee joint and consequently cause relative sliding of suspension cuffs at human-robot interface.

TABLE I. MAXIMUM NORMATIVE GAIT MEASURES OF WALKING [6]

| Joint | Angular Speed (RPM) | Moment (Nm/kg) | Power (W/kg) |
|-------|---------------------|----------------|--------------|
| Hip | 35 | 1.2 | 1 |
| Knee | 60 | 0.5 | 0.9 |
| Ankle | 38 | 1.8 | 3.4 |

B. Functional Considerations

Drive selection for the LEE robot mainly depends on the kinematic and dynamic requirements of the user based on nature of activities carried out. If the LEE robot is designed to support walking, the clinical gait analysis (CGA) data from biomechanical studies serve as a suitable reference for estimating ranges of motion, angular speed, torque, and power requirements for each of the joints. Table I include maximum normative measurements of walking gait data based on inverse dynamic models [6]. However, when considering limitations of the actuator technologies a suitable compromise has to be reached in determining the optimum power assist ratio of the exoskeleton robot.

The LEE robot is planned to be rearranged to suit users with wider range of mobility requirements. Thus, a modular design approach should be adopted for the development of its independent sub-systems such as powering system, control system, and structural system. In addition, mechanisms and connecting links should be adjustable to fit humans with varying anthropometric measurements. As such, a modular LEE robot can serve as a universal platform to test alternative powering and controlling strategies and minimize lead time for evaluations. However, attempts to adapt exoskeleton for different functional requirements and operational modes may increase design complexity.

III. RELATED WORK

Hip exoskeleton robots with multiple-DoF can be identified in literature. BLEEX [7] include a three DoF system with non-conforming AoR to support rotation about the transverse plane. Alternatively, HEXAR [8] uses a series chain structure with four hinged joints and BLERE [2] employs a curved slider to align the internal/external rotation axis. WPAH [9] uses a six-DoF parallel mechanism to facilitate complete hip movements using a combination of universal, spherical and prismatic joints. However, all such solutions resulted in bulky and complex articulated systems.

In order to minimize restrictions for achieving natural knee movements various mechanisms have been proposed. BLERE and AKJ [3] use cam-based slider mechanisms to match moving AoR. The designs are rugged and compact but performance is impeded by higher frictional losses. The ACJ [10] alternatively uses a five-bar link mechanism with two DoF to match trajectory of AoR. The link lengths should however be adjusted to match the individual requirements of the user. Similarly, a four-bar link system has been presented in [11], but lacks hardware evidence as proof of concept. The iT-Knee [12] and AssistON-Knee [13] are of two self-adjusting knee joint mechanisms that facilitate even the slight movements within knee complex to ameliorate misalignment issues over the anatomical planes. However, proposed solutions are complex and heavy for everyday use.

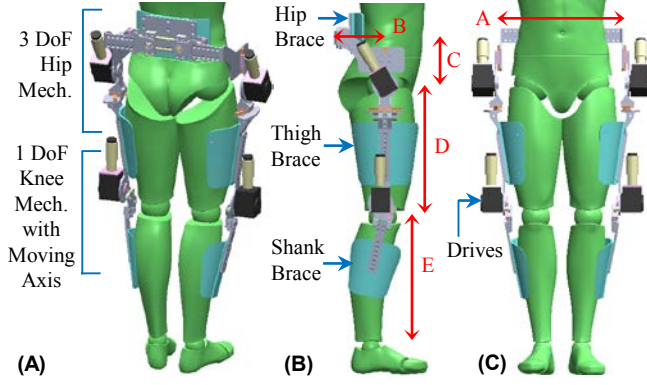


Figure 3. CAD model of Anthro-X fitted on a 3D scanned 50th percentile male subject: (A) side view, (B) front view, (C) back view.

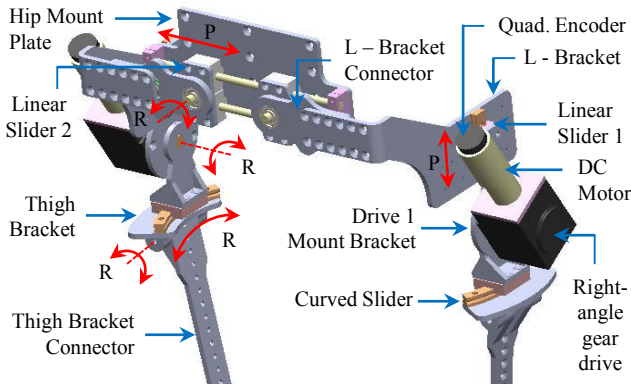


Figure 4. 3-DoF hip mechanism with joint axes mapping technology.

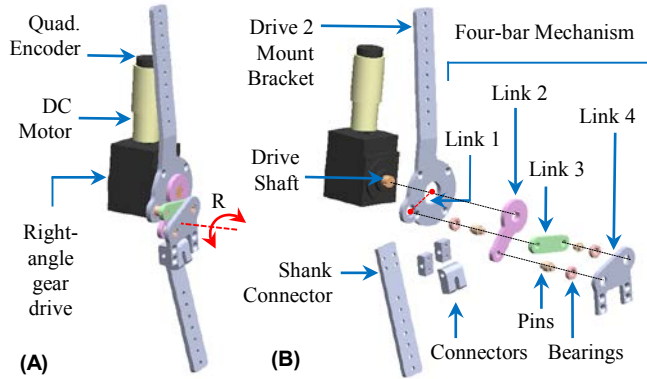


Figure 5. 1-DoF knee mechanism with moving AoR technology: (A) assembly, (B) exploded view.

TABLE II. RANGES OF MOTION OF HUMAN [4] AND EXOSKELETON

| Joint | Sagittal Plane | | Frontal Plane | | Transverse Plane | |
|-------|---------------------------------|------------------------------|---------------------------|---------------------------|-----------------------------------|--------------------------------|
| | Hum. | Exo. | Hum. | Exo. | Hum. | Exo. |
| Hip | -30 ~ 135 (Ext. ~ Flex.) | -25 ~ 35 (Ext. ~ Flex.) | -30 ~ 50 (Add. ~ Abd.) | -10 ~ 10 (Add. ~ Abd.) | -45 ~ 60 (Int-rot. ~ Ext-rot.) | 5 ~ 5 (Int-rot. ~ Ext-rot.) |
| Knee | -10 ~ 140 (Hy-Ext. ~ Flex.) | -5 ~ 90 (Hy-Ext. ~ Flex.) | N/A | N/A | N/A | N/A |
| Ankle | -20 ~ 50 (D-Flex. ~ P-Flex.) | Free | -30 ~ 20 (Inv. ~ Eve.) | Fixed | -35 ~ 50 (Int-rot. ~ Ext-rot.) | Fixed |

IV. DESIGN OF ANTHRO-X

Anthro-X is designed to support basic motions, as well as walking and lifting tasks. Here, mechanisms were developed to generate human like motions at hip and knee (See Fig. 3(A)). It is a bilateral system, where sagittal plane motions are powered by electrical actuators and other DoF are passively stabilized. In order to minimize interference at the human-robot interface, proposed structural systems and mechanisms strictly adhere to anthropomorphic architecture. The ankle joint of Anthro-X presently include a hinged joint with one DoF to transfer weight of LEE robot to the ground. Therefore, user is relieved from bearing load. Development of Anthro-X is mainly accomplished in several steps such as design of structural system, hip mechanism (See Fig. 4), knee mechanism (See Fig. 5) and controller hardware.

A. Design of Structural System

In order maximize maneuverability and reduce inertia, a lightweight structural system has been developed. The structure closely follow body contours of lower extremity from pelvic to foot segments (See Fig. 3(B) and 3(C)). A computer-aided design (CAD) model of a 3D scanned 50th percentile male subject was prepared to achieve the near accurate shape. In addition, provisions are kept to adjust the link lengths according to available anthropometry data [14]. This is achieved by introducing an array of holes along each of the links. The nominal lengths and adjustment ranges for A, B, C, D and E measures are 397 ± 50 , 197 ± 20 , 140 ± 50 , 424 ± 50 and 422 ± 50 mm respectively. However, minimum length adjustment or spacing between two holes is set to 10 mm. Table II includes ranges of motion of human [4] and exoskeleton. Mechanical limits were used to ensure safety of the user. All structural parts were fabricated using aluminium alloy as the material has high strength-to-weight ratio. Pins were made of alloy steel to enhance durability.

B. Design of Hip Mechanism

In order to correctly map the hip joint AoR, two linear guides, one curved guide and several hinges were introduced to the hip joint mechanism (See Fig. 4). Flexion/extension is achieved by directly coupling drive shaft through a hinged joint. The Drive 1 Mount Bracket is free to move over Linear Slider 1 to maintain axis alignment during abduction/adduction. An L-Bracket is used to mount the Linear Slider 1 (MGN15), which is then hinged on the Hip Mount Plate. The hip mechanism is mounted on the lower back of the human using Hip Mount Plate via a suspension cuff. L-Bracket Connector is mainly used to adjust the width of the mechanism to obtain a correct fit. The internal/external rotation axis is correctly mapped using a Curved Slider or arc guide (HCR12A+60/100R) having 100 mm radius. The hip mechanism is also connected to the thigh of the human using Thigh Bracket Connector via a suspension cuff. The Curved Slider mounted on the Thigh Bracket facilitates rotation of thigh with respect to the Drive 1 Mount Bracket.

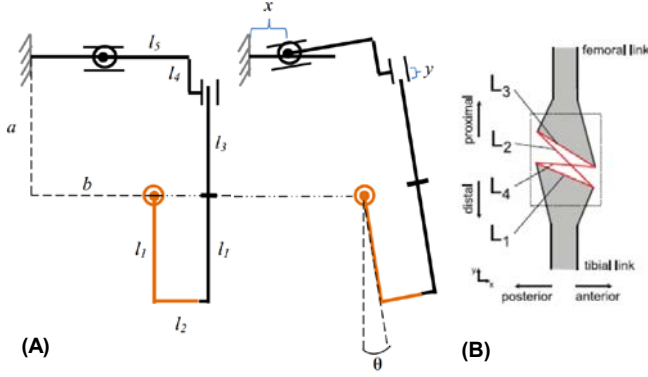


Figure 6. Models for joint mechanisms: (A) simplified model of hip mechanism, (B) four-bar link system by [11] to map moving AoR of knee.

Accordingly the proposed hip joint mechanism has the following technical characteristics.

- No. of links (N) – 6
- No. of joints (j) – 5
- No. of freedoms (f) – 3.5

Governing formula for mobility analysis in 3D reads as,

$$M = 6(N - I - j) + \sum_{i=1}^j f_i \quad (1)$$

The total DoF (M) of hip joint mechanism from (1) is determined to be 3.5. As such, the rigid articulated system pose no restrictions to reproduce natural hip motions. The rail lengths of the linear guides were determined according to the displacement exhibited by each slider upon abduction/adduction. Abduction and adduction angles was limited to 10^0 to maintain compactness of the mechanism. A simplified version of hip joint mechanism is presented to describe the working principle of the new design (See Fig. 6(A)). Here, ' a ' is the vertical distance between the upper linear guide and the human hip joint. ' b ' is the horizontal distance between the midpoint of the upper ' l ' linear guide and the hip joint. ' l_1 ' represent the distance between human hip joint to the human-robot interface at the thigh. ' l_2 ' is the radius of the arc guide mounted at the lower link of the hip mechanism. ' l_3 ', ' l_4 ' and ' l_5 ' gives the corresponding link lengths of the hip mechanism. Where, ' x ' and ' y ' represent the displacement of the upper and lower linear guides along the rails respectively. ' θ ' gives rotation angle over the frontal plane, such as abduction and adduction. Using geometric method, the formulas for x and y displacements were then derived.

$$x = b - a \tan \theta - (l_5 - l_2) \tan \theta \sin \theta - (l_5 - l_2) \cos \theta \quad (2)$$

$$y = \frac{a}{\cos \theta} - (l_5 - l_2) \tan \theta - l_3 - l_4 \quad (3)$$

For a 50th percentile male subject [14], the reference lengths for a , b , l_2 , l_3 , l_4 and l_5 parameters were identified to be 150 mm, 90 mm, 100 mm, 80 mm, 70 mm and 145 mm. The displacement of x and y for 10^0 of abduction and -10^0 of adduction were determined using (2) and (3).

Considering the adjustability for users with different body sizes and the length of the linear guides, the rail length of the upper linear guide was taken as 220 mm, allowing 90 mm of displacement for both the right and left side. The rail length of the lower linear guide was taken as 80 mm allowing 40 mm of displacement. In order to eliminate unstable motions occurring at the linear sliders, elastic helical springs made of steel are installed. Neutral position of sliders were determined based on standing position of the lower extremity. Therefore, the proposed hip mechanism is capable of supporting all three DoF exceptionally.

C. Design of Knee Mechanism

In a previous study by [11], a four-bar linkage system was proposed (See Fig. 6(B)) to provide a polycentric motion similar to that of a human knee joint where the instantaneous center of rotation of linkage follows the predicted AoR of the biological knee. In practical terms this is the imaginary point where linkages L_2 and L_4 intersect each other. However, except for the theoretical model, a mechanism based on the above notion has not been realized.

Hence, this study attempted to build on the knowledge base and introduce a novel mechanism for the knee joint (See Fig. 5(A)), which is compact and easy to fabricate. As such, Link 2 and Link 3 of the proposed knee mechanism (See Fig. 5(B)) directly corresponds to the L_2 and L_4 linkages of the four-bar system derived by [11]. The link lengths and their orientation were set identical to the geometric values determined by [11] using genetic algorithm based on relative fitness. In the proposed knee mechanism, Drive 2 Mount Bracket provides the connection between the thigh and the knee exoskeleton via a suspension cuff. Here, Drive 2 is also mounted on Drive 2 Mount Bracket and one end of Link 2 is fixed on to the Drive Shaft. The two ends of Link 3 are hinged on the Drive 2 Mount Bracket and Link 4 respectively. Opposite end of Link 2 is hinged on Link 4 to complete the four-bar system. The Shank Connector is fixed on Link 4 and also attached to the shank of the leg via a suspension cuff. This design aimed to minimize interference between biological knee and the robot, to improve user comfort by achieving axes alignment.

D. Design of Controller Hardware

In summary, the control system mainly consists of a microcontroller (Arduino Mega 2560), two motor controllers (Roboclaw 2 x 45A) and four DC brushed motors installed with planetary gear heads and quadrature encoders.

TABLE III. TECHNICAL CHARACTERISTICS OF ACTUATORS

| Joint | Motor Description | Reducer | Max. Output Torque | Max. Output Speed | Weight / Size |
|-------|------------------------------|-------------------------------|--------------------|-------------------|-----------------|
| Hip | 60 RPM Planetary Gear Motor | Right-angle drive (RAS60) 2:1 | 26.5 Nm | 30 RPM | 1.6 kg / 190 mm |
| Knee | 118 RPM Planetary Gear Motor | | 13.5 Nm | 59 RPM | x 69 mm |

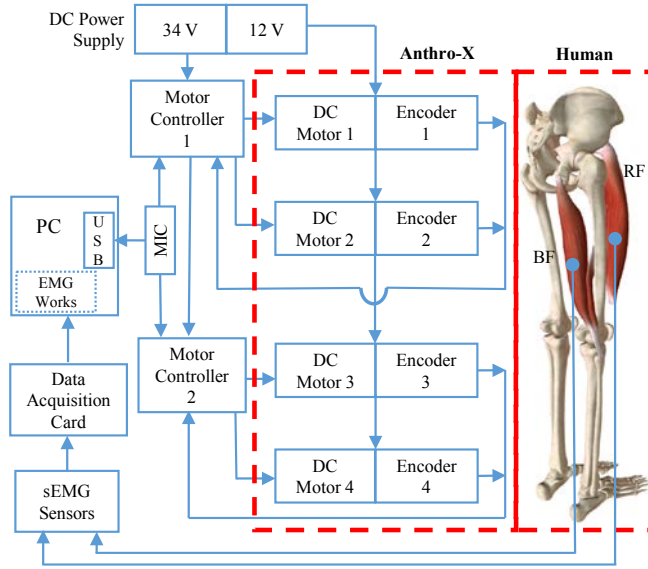


Figure 7. Experimental setup of Anthro-X including control diagram.

The selection of actuators was mainly influenced by speed of operation and power requirements at a given joint considering walking gait data [6]. The maximum assist ratio is selected as 30%. Smaller geometry, ease of control, high energy efficiency and lightweight are the other notable traits. In order to improve the compactness of the LEE robot, right angle gear drives were employed. A summary of the technical characteristics for the motors and gear reducers are given in Table III. Since LEE robot is to be used outdoors as an autonomous portable system, powering method is planned to be supported by a battery pack.

V. EVALUATION OF ANTHRO-X

Prototype of Anthro-X weighs approximately 15 kg without the battery pack, where the four actuators are measured to be 6.4 kg in total. The effectiveness of the proposed mechanisms for hip and knee joints were verified using several approaches. At first, qualitative feedback was obtained on kinematic conformity of mechanisms. Then, the control methodology was assessed to generate predetermined motion patterns. Finally, experimental evaluation of effects of power assistance based on muscle signals was conducted.

A. Experiment Setup

The motor controllers and DC motors are respectively powered with 34 V and 12 V DC power supply (See Fig. 7). The control signals for the motor controllers are generated using the microcontroller (MIC). DC Motor 1 and DC Motor 2 are used to drive the knee mechanisms of Anthro-X. Similarly, DC Motor 3 and DC Motor 4 are used to drive the hip mechanisms. However, only when knee exoskeleton is considered, Motor Controller 2 is set to inactive mode. The quadrature or incremental encoders provide the angular position feedback for controlling of the motors.

As per the control software, a PID controller is implemented. The controller was used to evaluate working

accuracy of joint mechanisms to produce flexion/ extension. Effectiveness of motion generation capability of was then determined by simulating predefined angular trajectories.

The muscle activation during the entire cycle was measured by wired surface electromyography (EMG) electrodes placed on bicep femoris (BF) and rectus femoris (RF) muscles on muscle bellies of both limbs using a 16-channel Bagnoli Desktop EMG systems. The raw EMG signals were measured and recorded using the Data Acquisition Card. EMG Works software was then used to calculate root mean square (RMS) values of EMG signals.

B. Experiment Protocol

Squatting exercise was selected to verify the fidelity of the proposed LEE robot for providing power assistance. EMG signals were then measured for the tests listed below.

- Case 1 - without the exoskeleton
- Case 2 - unpowered exoskeleton (Non-powered)
- Case 3 - externally powered exoskeleton (Powered)

In order to maintain simplicity, only the knee exoskeleton configuration of Anthro-X was considered for the study. In Case 3, when exoskeleton is externally powered, a predefined angular motion pattern corresponding to squatting action is fed into motors. Each of the tests were conducted for a period of 60 seconds with an ascent-descent cycle of four seconds that ranged over a 0 to 90° knee angle. A 50th percentile male subject (37 years, 72 kg and 178 cm) was selected to conduct above mentioned tests. Five-minute rest was provided in between tests to relax muscle fatigue.

C. Results and Discussion

In order to assess kinematic conformity of Anthro-X, all DoF were set to operate in passive sense. Then, the user's mobility was judged by performing basic joint motions, such as flexion/extension, abduction/adduction, and internal/external rotation, etc. (See Fig. 8). Overground and treadmill walking were also performed at 1.3 m/s without experiencing any undue restrictions or abnormal movements.

A predefined sinusoidal waveform was fed into the microcontroller and output angular motions of the joints were measured from the feedback signals of the encoders. Observed joint angles of Anthro-X shows good conformance with the input sinusoidal waveform for both hip and knee joints (See Fig. 9(A) & (B)).



Figure 8. Evaluation of kinematic conformity: (A) flexion/extension, (B) abduction/adduction, (C) internal/external rotation, (D) squatting.

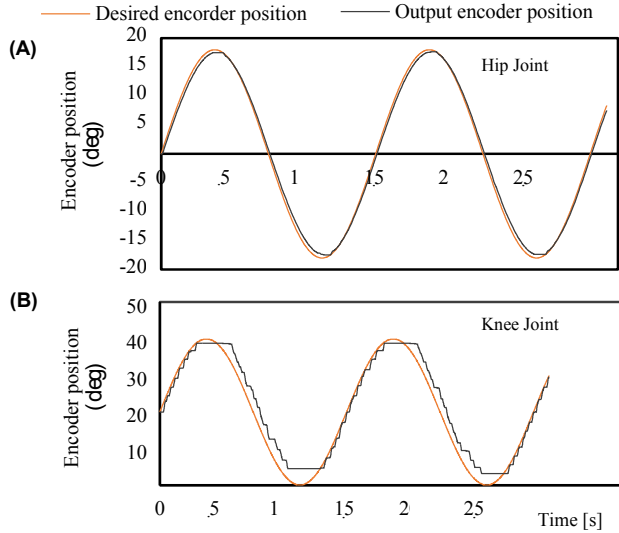


Figure 9. Responses to sinusoidal waveform input: (A) hip, (B) knee.

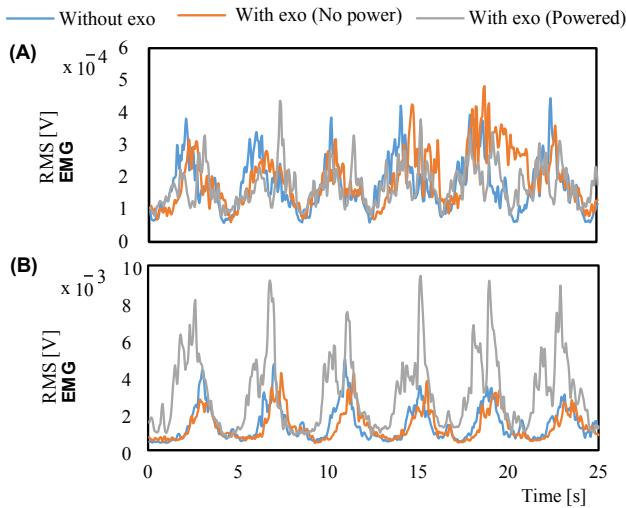


Figure 10. RMS EMG on left limb for first six squ. cycles: (A) BF, (B) RF.

For the first six squatting cycles (See Fig. 10(A)), in comparison to the case of ‘without the exoskeleton’, the BF muscles show a decrease in RMS EMG values when wearing the ‘non-powered exoskeleton’. The resistance provided by motors and gear drives have possibly assisted the limb muscles to lower the body weight. During the first six squatting cycle, RMS values of the BF muscles are similar for ‘non-powered and powered exoskeletons’. The peak RMS EMG values with ‘powered exoskeleton’ is generally lesser than the case of ‘without the exoskeleton’. However the peaks were registered at different time intervals during the squatting cycle.

The response of RF muscles during the first six squatting cycles (See Fig. 10(B)) are similar for ‘non-powered and powered exoskeletons’. However, peak RMS EMG values with ‘powered exoskeleton’ shows a drastic increase. This can be caused by isotonic contraction happening in the RF

muscles at the beginning of the squatting cycle as the muscles try to dampen the torque generated by the drive motor of knee joint mechanism. By adopting an impedance control strategy as opposed to position control method may provide favorable solution to remedy this issue.

VI. CONCLUSION

This paper presents an anthropomorphic LEE robot with two novel mechanisms to follow natural hip and knee movements. Proposed mechanisms are capable of providing power assistance over the sagittal plane and joint axes of rotations are also accurately mapped to achieve higher level of kinematic conformity. As future work, Anthro-X can be further developed to provide motion assistance for walking and/or to conduct rehabilitation exercises of hip and knee.

ACKNOWLEDGMENT

Authors are thankful for the assistance provided by resource personnel at Die and Mould Facilitation Center at University of Moratuwa. Authors also acknowledge the support given by Senate Research Council of University of Moratuwa, Sri Lanka (Grant No. - SRC/CAP/2014/08).

REFERENCES

- [1] A. J. Young and D. P. Ferris, “State of the Art and Future Directions for Lower Limb Robotic Exoskeletons,” *IEEE Trans. Neural Syst. Rehabil. Eng.*, vol. 25, no. 2, pp. 171–182, Feb. 2017.
- [2] W. Yang, C. Yang, and Q. Wei, “Design of an anthropomorphic lower extremity exoskeleton with compatible joints,” in *IEEE Int. Conf. on Rob. and Bio.*, 2014, pp. 1374–1379.
- [3] D. Wang, K.-M. Lee, J. Guo, and C.-J. Yang, “Adaptive Knee Joint Exoskeleton Based on Biological Geometries,” *IEEE/ASME Trans. Mechatronics*, vol. 19, no. 4, pp. 1268–1278, Aug. 2014.
- [4] D. A. Neumann, *Kinesiology of the musculoskeletal system: foundations for physical rehabilitation*, 2nd ed. Mosby, 2002.
- [5] T. R. D. Joseph Hamill, Kathleen M. Knutzen, *Biomechanical basis of human movement*, 4th ed. Wolters Kluwer, 2015.
- [6] B. R. Umberger and P. E. Martin, “Mechanical power and efficiency of level walking with different stride rates,” *J. Exp. Biol.*, vol. 210, no. 18, pp. 3255–3265, Sep. 2007.
- [7] A. B. Zoss, H. Kazerooni, and A. Chu, “Biomechanical design of the Berkeley lower extremity exoskeleton (BLEEX),” *IEEE/ASME Trans. Mechatronics*, vol. 11, no. 2, pp. 128–138, Apr. 2006.
- [8] D. Lim et al., “Development of a lower extremity exoskeleton robot with a quasi-anthropomorphic design approach for load carriage,” in *IEEE/RSJ Int. Conf. on Int. Rob. and Sys.*, 2015, pp. 5345–5350.
- [9] Y. Yu and H. Tao, “A parallel mechanism and a control strategy based on interactive force using on hip joint power assist,” *Int. J. Mechatronics Autom.*, vol. 4, no. 1, p. 39, 2014.
- [10] Jiun-Yih Kuan, K. A. Pasch, and H. M. Herr, “Design of a knee joint mechanism that adapts to individual physiology,” *Int. Conf. on IEEE Engineering in Medicine and Biology Society*, 2014, pp. 2061–2064.
- [11] J. M. B. Bertomeu et al., “Development of a hinge compatible with the kinematics of the knee joint,” *Prosthet. Orthot. Int.*, vol. 31, no. 4, pp. 371–383, Dec. 2007.
- [12] L. Saccarese, I. Sarakoglou, and N. G. Tsagarakis, “iT-Knee: An exoskeleton with ideal torque transmission interface for ergonomic power augmentation,” in *IEEE/RSJ Int. Conf. on Int. Rob. and Sys.*, 2016, pp. 780–786.
- [13] B. Celebi, M. Yalcin, and V. Patoglu, “AssistOn-Knee: A self-aligning knee exoskeleton,” in *IEEE/RSJ Int. Conf. on Int. Rob. and Sys.*, 2013, pp. 996–1002.
- [14] A. Tilley, *The Measure of man and woman*. Watson-Guptill, 1993.